Eur. Phys. J. C 31, 139–147 (2003)
Digital Object Identifier (DOI) 10.1140/epjc/s2003-01350-x

THE EUROPEAN PHYSICAL JOURNAL C

Measurement of the $e^+e^- \to W^+W^-\gamma$ cross-section and limits on anomalous quartic gauge couplings with DELPHI

The DELPHI Collaboration

J. Abdallah[25], P. Abreu[22], W. Adam[51], P. Adzic[11], T. Albrecht[17], T. Alderweireld[2], R. Alemany-Fernandez[8], T. Allmendinger[17], P.P. Allport[23], U. Amaldi[29], N. Amapane[45], S. Amato[48], E. Anashkin[36], A. Andreazza[28], S. Andringa[22], N. Anjos[22], P. Antilogus[27], W-D. Apel[17], Y. Arnoud[14], S. Ask[26], B. Asman[44], J.E. Augustin[25], A. Augustinus[8], P. Baillon[8], A. Ballestrero[46], P. Bambade[20], R. Barbier[27], D. Bardin[16], G. Barker[17], A. Baroncelli[39], M. Battaglia[8], M. Baubillier[25], K-H. Becks[53], M. Begalli[6], A. Behrmann[53], E. Ben-Haim[20], N. Benekos[32], A. Benvenuti[5], C. Berat[14], M. Berggren[25], L. Berntzon[44], D. Bertrand[2], M. Besancon[40], N. Besson[40], D. Bloch[9], M. Blom[31], M. Bluj[52], M. Bonesini[29], M. Boonekamp[40], P.S.L. Booth[23], G. Borisov[21], O. Botner[49], B. Bouquet[20], T.J.V. Bowcock[23], I. Boyko[16], M. Bracko[43], R. Brenner[49], E. Brodet[35], P. Bruckman[18], J.M. Brunet[7], L. Bugge[33], P. Buschmann[53], M. Calvi[29], T. Camporesi[8], V. Canale[38], F. Carena[8], N. Castro[22], F. Cavallo[5], M. Chapkin[42], Ph. Charpentier[8], P. Checchia[36], R. Chierici[8], P. Chliapnikov[42], J. Chudoba[8], S.U. Chung[8], K. Cieslik[18], P. Collins[8], R. Contri[13], G. Cosme[20], F. Cossutti[47], M.J. Costa[50], B. Crawley[1], D. Crennell[37], J. Cuevas[34], J. D'Hondt[2], J. Dalmau[44], T. da Silva[48], W. Da Silva[25], G. Della Ricca[47], A. De Angelis[47], W. De Boer[17], C. De Clercq[2], B. De Lotto[47], N. De Maria[45], A. De Min[36], L. de Paula[48], L. Di Ciaccio[38], A. Di Simone[39], K. Doroba[52], J. Drees[53,8], M. Dris[32], G. Eigen[4], T. Ekelof[49], M. Ellert[49], M. Elsing[8], M.C. Espirito Santo[22], G. Fanourakis[11], D. Fassouliotis[11,3], M. Feindt[17], J. Fernandez[41], A. Ferrer[50], F. Ferro[13], U. Flagmeyer[53], H. Foeth[8], E. Fokitis[32], F. Fulda-Quenzer[20], J. Fuster[50], M. Gandelman[48], C. Garcia[50], Ph. Gavillet[8], E. Gazis[32], R. Gokieli[8,52], B. Golob[43], G. Gomez-Ceballos[41], P. Goncalves[22], E. Graziani[39], G. Grosdidier[20], K. Grzelak[52], J. Guy[37], C. Haag[17], A. Hallgren[49], K. Hamacher[53], K. Hamilton[35], J. Hansen[33], S. Haug[33], F. Hauler[17], V. Hedberg[26], M. Hennecke[17], H. Herr[8], J. Hoffman[52], S-O. Holmgren[44], P.J. Holt[8], M.A. Houlden[23], K. Hultqvist[44], J.N. Jackson[23], G. Jarlskog[26], P. Jarry[40], D. Jeans[35], E.K. Johansson[44], P.D. Johansson[44], P. Jonsson[27], C. Joram[8], L. Jungermann[17], F. Kapusta[25], S. Katsanevas[27], E. Katsoufis[32], G. Kernel[43], B.P. Kersevan[8,43], A. Kiiskinen[15], B.T. King[23], N.J. Kjaer[8], P. Kluit[31], P. Kokkinias[11], C. Kourkoumelis[3], O. Kouznetsov[16], Z. Krumstein[16], M. Kucharczyk[18], J. Lamsa[1], G. Leder[51], F. Ledroit[14], L. Leinonen[44], R. Leitner[30], J. Lemonne[2], V. Lepeltier[20], T. Lesiak[18], W. Liebig[53], D. Liko[51], A. Lipniacka[44], J.H. Lopes[48], J.M. Lopez[34], D. Loukas[11], P. Lutz[40], L. Lyons[35], J. MacNaughton[51], A. Malek[53], S. Maltezos[32], F. Mandl[51], J. Marco[41], R. Marco[41], B. Marechal[48], M. Margoni[36], J-C. Marin[8], C. Mariotti[8], A. Markou[11], C. Martinez-Rivero[41], J. Masik[12], N. Mastroyiannopoulos[11], F. Matorras[41], C. Matteuzzi[29], F. Mazzucato[36], M. Mazzucato[36], R. Mc Nulty[23], C. Meroni[28], W.T. Meyer[1], E. Migliore[45], W. Mitaroff[51], U. Mjoernmark[26], T. Moa[44], M. Moch[17], K. Moenig[8,10], R. Monge[13], J. Montenegro[31], D. Moraes[48], S. Moreno[22], P. Morettini[13], U. Mueller[53], K. Muenich[53], M. Mulders[31], L. Mundim[6], W. Murray[37], B. Muryn[19], G. Myatt[35], T. Myklebust[33], M. Nassiakou[11], F. Navarria[5], K. Nawrocki[52], R. Nicolaidou[40], M. Nikolenko[16,9], A. Oblakowska-Mucha[19], V. Obraztsov[42], A. Olshevski[16], A. Onofre[22], R. Orava[15], K. Osterberg[15], A. Ouraou[40], A. Oyanguren[50], M. Paganoni[29], S. Paiano[5], J.P. Palacios[23], H. Palka[18], Th.D. Papadopoulou[32], L. Pape[8], C. Parkes[24], F. Parodi[13], U. Parzefall[8], A. Passeri[39], O. Passon[53], L. Peralta[22], V. Perepelitsa[50], A. Perrotta[5], A. Petrolini[13], J. Piedra[41], L. Pieri[39], F. Pierre[40], M. Pimenta[22], E. Piotto[8], T. Podobnik[43], V. Poireau[8], M.E. Pol[6], G. Polok[18], P. Poropat[47,†], V. Pozdniakov[16], N. Pukhaeva[2,16], A. Pullia[29], J. Rames[12], L. Ramler[17], A. Read[33], P. Rebecchi[8], J. Rehn[17], D. Reid[31], R. Reinhardt[53], P. Renton[35], F. Richard[20], J. Ridky[12], M. Rivero[41], D. Rodriguez[41], A. Romero[45], P. Ronchese[36], E. Rosenberg[1], P. Roudeau[20], T. Rovelli[5], V. Ruhlmann-Kleider[40], D. Ryabtchikov[42], A. Sadovsky[16], L. Salmi[15], J. Salt[50], A. Savoy-Navarro[25], U. Schwickerath[8], A. Segar[35], R. Sekulin[37], M. Siebel[53], A. Sisakian[16], G. Smadja[27], O. Smirnova[26], A. Sokolov[42], A. Sopczak[21], R. Sosnowski[52], T. Spassov[8], M. Stanitzki[17], A. Stocchi[20], J. Strauss[51], B. Stugu[4], M. Szczekowski[52], M. Szeptycka[52], T. Szumlak[19], T. Tabarelli[29], A.C. Taffard[23], F. Tegenfeldt[49], J. Timmermans[31], L. Tkatchev[16], M. Tobin[23], S. Todorovova[12], B. Tome[22], A. Tonazzo[29], P. Tortosa[50], P. Travnicek[12], D. Treille[8], G. Tristram[7], M. Trochimczuk[52], C. Troncon[28], M-L. Turluer[40], I.A. Tyapkin[16], P. Tyapkin[16], S. Tzamarias[11], V. Uvarov[42], G. Valenti[5], P. Van Dam[31], J. Van Eldik[8], A. Van Lysebetten[2], N. Ran Remortel[2], I. Van Vulpen[8], G. Vegni[28], F. Veloso[22], W. Venus[37], P. Verdier[27], V. Verzi[38], D. Vilanova[40], L. Vitale[47], V. Vrba[12], H. Wahlen[53], A.J. Washbrook[23], C. Weiser[17], D. Wicke[8], J. Wickens[2], G. Wilkinson[35], M. Winter[9], M. Witek[18], O. Yushchenko[42], A. Zalewska[18], P. Zalewski[52], D. Zavrtanik[43], V. Zhuravlov[16], N.I. Zimin[16], A. Zintchenko[16], M. Zupan[11]

[1] Department of Physics and Astronomy, Iowa State University, Ames IA 50011-3160, USA
[2] Physics Department, Universiteit Antwerpen, Universiteitsplein 1, 2610 Antwerpen, Belgium
and IIHE, ULB-VUB, Pleinlaan 2, 1050 Brussels, Belgium
and Faculté des Sciences, Univ. de l'Etat Mons, Av. Maistriau 19, 7000 Mons, Belgium
[3] Physics Laboratory, University of Athens, Solonos Str. 104, 10680 Athens, Greece
[4] Department of Physics, University of Bergen, Allégaten 55, 5007 Bergen, Norway
[5] Dipartimento di Fisica, Università di Bologna and INFN, Via Irnerio 46, 40126 Bologna, Italy
[6] Centro Brasileiro de Pesquisas Físicas, rua Xavier Sigaud 150, 22290 Rio de Janeiro, Brazil
and Depto. de Física, Pont. Univ. Católica, C.P. 38071 22453 Rio de Janeiro, Brazil
and Inst. de Física, Univ. Estadual do Rio de Janeiro, rua São Francisco Xavier 524, Rio de Janeiro, Brazil
[7] Collège de France, Lab. de Physique Corpusculaire, IN2P3-CNRS, 75231 Paris Cedex 05, France
[8] CERN, 1211 Geneva 23, Switzerland
[9] Institut de Recherches Subatomiques, IN2P3 – CNRS/ULP – BP20, 67037 Strasbourg Cedex, France
[10] Now at DESY-Zeuthen, Platanenallee 6, 15735 Zeuthen, Germany
[11] Institute of Nuclear Physics, N.C.S.R. Demokritos, P.O. Box 60228, 15310 Athens, Greece
[12] FZU, Inst. of Phys. of the C.A.S. High Energy Physics Division, Na Slovance 2, 180 40, Praha 8, Czech Republic
[13] Dipartimento di Fisica, Università di Genova and INFN, Via Dodecaneso 33, 16146 Genova, Italy
[14] Institut des Sciences Nucléaires, IN2P3-CNRS, Université de Grenoble 1, 38026 Grenoble Cedex, France
[15] Helsinki Institute of Physics, P.O. Box 64, 00014 University of Helsinki, Finland
[16] Joint Institute for Nuclear Research, Dubna, Head Post Office, P.O. Box 79, 101 000 Moscow, Russian Federation
[17] Institut für Experimentelle Kernphysik, Universität Karlsruhe, Postfach 6980, 76128 Karlsruhe, Germany
[18] Institute of Nuclear Physics,Ul. Kawiory 26a, 30055 Krakow, Poland
[19] Faculty of Physics and Nuclear Techniques, University of Mining and Metallurgy, 30055 Krakow, Poland
[20] Université de Paris-Sud, Lab. de l'Accélérateur Linéaire, IN2P3-CNRS, Bât. 200, 91405 Orsay Cedex, France
[21] School of Physics and Chemistry, University of Lancaster, Lancaster LA1 4YB, UK
[22] LIP, IST, FCUL – Av. Elias Garcia, 14-1^o, 1000 Lisboa Codex, Portugal
[23] Department of Physics, University of Liverpool, P.O. Box 147, Liverpool L69 3BX, UK
[24] Dept. of Physics and Astronomy, Kelvin Building, University of Glasgow, Glasgow G12 8QQ
[25] LPNHE, IN2P3-CNRS, Univ. Paris VI et VII, Tour 33 (RdC), 4 place Jussieu, 75252 Paris Cedex 05, France
[26] Department of Physics, University of Lund, Sölvegatan 14, 223 63 Lund, Sweden
[27] Université Claude Bernard de Lyon, IPNL, IN2P3-CNRS, 69622 Villeurbanne Cedex, France
[28] Dipartimento di Fisica, Università di Milano and INFN-MILANO, Via Celoria 16, 20133 Milan, Italy
[29] Dipartimento di Fisica, Univ. di Milano-Bicocca and INFN-MILANO, Piazza della Scienza 2, 20126 Milan, Italy
[30] IPNP of MFF, Charles Univ., Areal MFF, V Holesovickach 2, 180 00, Praha 8, Czech Republic
[31] NIKHEF, Postbus 41882, 1009 DB Amsterdam, The Netherlands
[32] National Technical University, Physics Department, Zografou Campus, 15773 Athens, Greece
[33] Physics Department, University of Oslo, Blindern, 0316 Oslo, Norway
[34] Dpto. Fisica, Univ. Oviedo, Avda. Calvo Sotelo s/n, 33007 Oviedo, Spain
[35] Department of Physics, University of Oxford, Keble Road, Oxford OX1 3RH, UK
[36] Dipartimento di Fisica, Università di Padova and INFN, Via Marzolo 8, 35131 Padua, Italy
[37] Rutherford Appleton Laboratory, Chilton, Didcot OX11 OQX, UK
[38] Dipartimento di Fisica, Università di Roma II and INFN, Tor Vergata, 00173 Rome, Italy
[39] Dipartimento di Fisica, Università di Roma III and INFN, Via della Vasca Navale 84, 00146 Rome, Italy
[40] DAPNIA/Service de Physique des Particules, CEA-Saclay, 91191 Gif-sur-Yvette Cedex, France
[41] Instituto de Fisica de Cantabria (CSIC-UC), Avda. los Castros s/n, 39006 Santander, Spain
[42] Inst. for High Energy Physics, Serpukov P.O. Box 35, Protvino, (Moscow Region), Russian Federation
[43] J. Stefan Institute, Jamova 39, 1000 Ljubljana, Slovenia
and Laboratory for Astroparticle Physics, Nova Gorica Polytechnic, Kostanjeviska 16a, 5000 Nova Gorica, Slovenia,
and Department of Physics, University of Ljubljana, 1000 Ljubljana, Slovenia
[44] Fysikum, Stockholm University, Box 6730, 113 85 Stockholm, Sweden
[45] Dipartimento di Fisica Sperimentale, Università di Torino and INFN, Via P. Giuria 1, 10125 Turin, Italy
[46] INFN,Sezione di Torino, and Dipartimento di Fisica Teorica, Università di Torino, Via P. Giuria 1, 10125 Turin, Italy
[47] Dipartimento di Fisica, Università di Trieste and INFN, Via A. Valerio 2, 34127 Trieste, Italy
and Istituto di Fisica, Università di Udine, 33100 Udine, Italy
[48] Univ. Federal do Rio de Janeiro, C.P. 68528 Cidade Univ., Ilha do Fundão 21945-970 Rio de Janeiro, Brazil
[49] Department of Radiation Sciences, University of Uppsala, P.O. Box 535, 751 21 Uppsala, Sweden
[50] IFIC, Valencia-CSIC, and D.F.A.M.N., U. de Valencia, Avda. Dr. Moliner 50, 46100 Burjassot (Valencia), Spain
[51] Institut für Hochenergiephysik, Österr. Akad. d. Wissensch., Nikolsdorfergasse 18, 1050 Vienna, Austria
[52] Inst. Nuclear Studies and University of Warsaw, Ul. Hoza 69, 00681 Warsaw, Poland
[53] Fachbereich Physik, University of Wuppertal, Postfach 100 127, 42097 Wuppertal, Germany
[†] deceased

Received: 21 July 2003 / Revised version: 2 September 2003 /
Published online: 10 October 2003 – © Springer-Verlag / Società Italiana di Fisica 2003

Abstract. $W^+W^-\gamma$ production at LEP2 is studied using data collected with the DELPHI detector at centre-of-mass energies between 189 GeV and 209 GeV, corresponding to an integrated luminosity of about 600 pb^{-1}. Cross-sections are measured for the production of W^+W^- with a hard, central and isolated photon in the final state, and are found to be compatible with the Standard Model prediction. The photon energy spectra are used to derive limits on anomalous contributions to the $W^+W^-Z^0\gamma$ and $W^+W^-\gamma\gamma$ vertices.

1 Introduction

W^+W^- production at LEP has been extensively analysed, with both the total cross-section and the Triple Gauge boson Coupling (TGC) structure showing good agreement with the Standard Model (SM) predictions [1]. The high centre-of-mass energy and large data sample available also make it possible to study in detail the events in which a photon is produced together with the $W^\pm$ pair. This paper presents the measurement of the cross-section for $W^\pm$ pair production with a hard, central and isolated photon in the final state.

The Quartic Gauge boson Couplings (QGCs), $W^+W^-Z^0\gamma$ and $W^+W^-\gamma\gamma$, give rise to 4-fermion+γ final states but their contribution at LEP2 energies is expected to be only about 3 fb in the framework of the SM. At present energies, these final states result mainly from initial state radiation (ISR) in W^+W^- production, from radiation from the final state charged fermions (FSR) or from the intermediate $W^\pm$ boson system (WSR). The requirement that the photons be isolated with respect to the final state charged fermions and the incoming electron/positron beams suppresses phase space regions almost entirely dominated by ISR and FSR, and enhances possible effects from anomalous QGCs.

Deviations from the SM predictions in these final states could imply the presence of contact interaction contributions to the QGCs, signalling new physics whose direct effects are inaccessible at present energies and could be masked in the TGC measurements. The QGC analysis is therefore performed in terms of "genuine" quartic gauge couplings, *i.e.* excluding those which also give rise to triple gauge couplings.

Several different parameterizations of the genuine anomalous QGCs have been given in the literature [2,3]. In this paper, we follow the analysis of Denner *et al* [3], which defines five non-SM Lagrangian operators which conserve electromagnetic gauge invariance and a custodial $SU(2)_c$ symmetry, and which can give contributions to the quartic gauge boson vertex. The contributions to the total Lagrangian density are:

$$\mathcal{L}_c = -\tfrac{\pi\alpha}{4\Lambda^2} a_c F_{\alpha\mu} F^{\alpha\nu} (\overrightarrow{W}_\nu . \overrightarrow{W}^\mu) \,,$$

$$\mathcal{L}_0 = -\tfrac{\pi\alpha}{4\Lambda^2} a_0 F_{\alpha\beta} F^{\alpha\beta} (\overrightarrow{W}_\mu . \overrightarrow{W}^\mu) \,,$$

$$\tilde{\mathcal{L}}_0 = -\tfrac{\pi\alpha}{4\Lambda^2} \tilde{a}_0 F_{\alpha\beta} \tilde{F}^{\alpha\beta} (\overrightarrow{W}_\mu . \overrightarrow{W}^\mu) \,,$$

$$\mathcal{L}_n = -\tfrac{\pi\alpha}{4\Lambda^2} a_n \epsilon_{ijk} W^{(i)}_{\mu\alpha} W^{(j)}_{\nu} W^{(k)\alpha} F^{\mu\nu} \,,$$

$$\tilde{\mathcal{L}}_n = -\tfrac{\pi\alpha}{4\Lambda^2} \tilde{a}_n \epsilon_{ijk} W^{(i)}_{\mu\alpha} W^{(j)}_{\nu} W^{(k)\alpha} \tilde{F}^{\mu\nu} \,,$$

where the field strengths $F_{\mu\nu}$ and $\overrightarrow{W}_{\mu\nu}$ are defined by $F_{\mu\nu} = \partial_\mu A_\nu - \partial_\nu A_\mu$ and $\overrightarrow{W}_{\mu\nu} = \partial_\mu \overrightarrow{W}_\nu - \partial_\nu \overrightarrow{W}_\mu$, respectively, and $2\tilde{F}_{\mu\nu} = \epsilon_{\mu\nu\rho\sigma} F^{\rho\sigma} (\epsilon^{0123} = 1)$; A_μ is the photon field and $\sqrt{2}\overrightarrow{W}_\mu = \big((W^+ + W^-)_\mu \,,\, i(W^+ - W^-)_\mu \,,\, \frac{\sqrt{2}}{\cos\theta_W} Z_\mu\big)$ is the triplet of massive gauge bosons. The parameter Λ has units of energy and represents the scale at which new physics would become manifest, and a_c, a_0, $\tilde{a}_0$, a_n and $\tilde{a}_n$ are dimensionless parameters determining the separate contributions of each operator.

The first three of these operators contribute to the $W^+W^-\gamma\gamma$ coupling and the last two to the $W^+W^-Z^0\gamma$ coupling. $\mathcal{L}_c$ and $\mathcal{L}_0$ conserve C and P, $\tilde{\mathcal{L}}_n$ conserves CP but not the separate symmetries, $\tilde{\mathcal{L}}_0$ conserves only C and $\mathcal{L}_n$ conserves only P. All these anomalous couplings change not only the total $W^+W^-\gamma$ cross-section but also modify the energy spectra of the observed photons. In this paper we determine the possible separate contributions of each of these operators to $WW\gamma$ production at LEP.

The results are based on the data collected with the DELPHI detector at centre-of-mass energies between 189 and 209 GeV, corresponding to a total integrated luminosity of about 600 pb^{-1}. Results from the other LEP collaborations on the $W^+W^-\gamma$ final state and on anomalous QGCs can be found in [4,5].

2 Data samples

The data studied in this paper were collected in the LEP runs of 1998 to 2000. In 1998, DELPHI collected a total luminosity of 154 pb^{-1} at 189 GeV, and in 1999 integrated luminosities of 26, 77, 84 and 41 pb^{-1} were recorded at 192, 196, 200 and 202 GeV, respectively. In 2000, the centre-of-mass energies ranged from 200 to 209 GeV; for part of the year, DELPHI suffered from a problem in one of the 12 sectors of its main tracking device (the TPC) and, although the effect on the present analysis is small, these data were analysed separately to isolate any systematic difference. The 2000 data with the TPC fully operational correspond to 161 pb^{-1}, and the second set of data to 58 pb^{-1}, both with average centre-of-mass energies of 206 GeV.

The DELPHI apparatus and performance are described in detail in [6,7]. The tracking system of DELPHI consisted

of a Time Projection Chamber (TPC) and a Vertex Detector (VD), and was supplemented by extra tracking detectors, the Inner and Outer Detectors in the barrel region, and two Forward Chambers. It was embedded in a magnetic field of 1.2 T, aligned parallel to the beam axis. The electromagnetic calorimetry consisted of the High density Projection Chamber (HPC) in the barrel region, the Forward Electromagnetic Calorimeter (FEMC) and the Small angle Tile Calorimeter in the forward regions. The regions between the HPC and the FEMC and between HPC modules were instrumented by scintillators fitted with lead converters so that photons could also be tagged there. The hadronic calorimeter covered 98% of the total solid angle and the whole detector was surrounded by muon drift chambers. The major hardware change with respect to the description in [7] was the inclusion of the Very Forward Tracker [8] which extended the coverage of the Vertex Detector down to a polar angle of 11°. Together with new tracking algorithms and alignment and calibration procedures, this led to an improved track reconstruction efficiency in the forward regions of DELPHI. The tracking algorithms for the barrel part of DELPHI were also changed to recuperate efficiency in the damaged TPC sector.

The final states considered as $W^+W^-\gamma$ candidates were $q\bar{q}q\bar{q}\gamma$ and $q\bar{q}l\nu\gamma$, where q represents a quark jet and $l \equiv e, \mu, \tau$. Events corresponding to SM processes with hadronic final states were fully simulated for the separate data samples. All the 4-fermion final states (including neutral and charged currents) were generated with the setup described in [9], based on the WPHACT [10] generator. WPHACT was interfaced with YFSWW [11] to include radiative corrections in the Double Pole Approximation (DPA) approach and to perform ISR corrections (including also ISR/WSR interference – of special relevance for the final states studied in this paper), while PYTHIA [12] modelled the FSR for quarks and TAUOLA [13] and PHOTOS [14] modelled the FSR for the charged leptons. The $q\bar{q}(\gamma)$ final states were generated with KK2f [15]. For all signal and background processes, the jet fragmentation and hadronization was simulated according to the DELPHI tuned JETSET/PYTHIA model [16]. All other SM background processes were found to give negligible contributions to the selected samples.

Samples of $W^+W^-\gamma$ with anomalous Quartic Gauge Couplings were simulated using weighted events from EEWWG [17]. This includes a full $O(\alpha)$ calculation of ISR, WSR and QGC diagrams but not FSR ones; it was interfaced with PYTHIA to simulate the fragmentation, hadronization and FSR from the charged fermions and with the EXCALIBUR radiator function [18] to describe collinear ISR. It was checked that the predictions of EEWWG without anomalous QGCs were compatible with the contribution of the W^+W^- production tree-level diagrams (CC03) [19] from the WPHACT samples, including DPA corrections but excluding FSR effects, in the region studied. The effect of the collinear ISR is to reduce the effective centre-of-mass energy and consequently lower the expected cross-section for visible photons. The inclusion of the radiative effects from EXCALIBUR in addition to the ISR matrix element in EEWWG results in a small double counting of the ISR and of its interference with the other contributing processes; however, in the analysis, most of this is removed by the use of a subtraction procedure in the event weights, as described below.

The EEWWG program is primarily intended to describe anomalous QGC effects for on-shell $W^+W^-\gamma$ production: the anomalous signal to be added to the SM was defined by applying to each EEWWG event a weight $w = w(a_c, a_0, \tilde{a}_0, a_n, \tilde{a}_n) - w(\mathbf{0})$, defined as the difference between the matrix element squared calculated with anomalous couplings $\mathbf{a} \neq \mathbf{0}$ and the SM calculation ($\mathbf{a} = \mathbf{0}$) [1]. Samples of $W^+W^-\gamma$ in all final states were generated with EEWWG and fully simulated at centre-of-mass energies of 189, 198 and 206 GeV. The WPHACT samples were used to define the SM signal to be measured and, in the analysis of anomalous QGCs, the extra contribution from EEWWG was added with the weights defined above. Both the SM and the anomalous QGCs cross-sections obtained in this way were found to be compatible with those obtained using RacoonWW [3].

3 Event selection

The general event reconstruction was based on that used by DELPHI for analysis of the process $e^+e^- \to W^+W^-$ [20], but with a less restrictive photon identification in order to enrich the $W^+W^-\gamma$ sample.

The reconstruction of photons in DELPHI was done in several steps, starting from the showers in the electromagnetic calorimeters. In the barrel, the procedure described in [7] was followed. Further "loose" showers, close to the HPC divisions, were accepted even if they failed the transverse shower profile criteria (and also the longitudinal one, for showers of energy exceeding 25 GeV). In the forward region, all STIC energy deposits with polar angle, θ, with respect to the beam direction satisfying $3° < \theta < 11°$ were taken to be photon candidates[2], while, for $\theta > 11°$, an algorithm was used to reduce the effects of the shower development in the detector material in front of the FEMC: electromagnetic deposits close in space in the FEMC were clustered together and the association with reconstructed charged particle tracks was used for electron/photon discrimination. Care was taken to exclude those tracks which were likely to come from the development of showers outside the calorimeter. Photons with two associated tracks were kept in the "loose" selection, but the "tight" selection required that no VD track elements, nor signals from different combinations of other tracking detectors (depending on the shower polar angle)

[1] Following [3], $\tilde{a}_0$ and $\tilde{a}_n$ were introduced in EEWWG by replacing $a_0 \to a_0 + i\ \tilde{a}_0$ and $a_n \to a_n + i\ \tilde{a}_n$ and the signs of a_0/Λ^2 and a_c/Λ^2 were reversed with respect to the ones in the original EEWWG code

[2] Energy depositions below 3° were discarded from the events, to avoid contamination from off-momentum beam electrons

be associated with the electromagnetic deposit. In addition, "loose" and "tight" photons were required to have a ratio between the electromagnetic energy and the total energy above 90% in the angular region around the cluster defined by $|\Delta\theta| < 15°$ and $|\Delta\phi| < \min(15°, 6° \cot\theta_{cluster})$, where ϕ is the azimuthal angle in the plane perpendicular to the beam direction and θ is the polar angle.

The identification of isolated photons in the $W^+W^-\gamma$ samples started from the photon candidates defined above and relied on a double cone centred around the photon axis, as explained below. Only isolated photons with energies above 5 GeV were considered.

The total energy inside a cone of 5° was associated to the photon, while, to ensure isolation, the energy between 5° and 15° was not permitted to exceed 1 GeV. These criteria were relaxed for tightly identified photons. In this case, no further association was done and only the external cone was considered. The corresponding angle, α, was varied according to the energy of the photon candidate (from 15° down to 3° for $E_\gamma > 90$ GeV), with the energy inside the cone allowed to be reduced proportionally to $\sin\alpha/\sin(15°)$. To enrich the FSR sample, identified muons and electrons coming from the $W^\pm$ were excluded from the energy counting within the photon external cone. All other charged particle tracks (not associated to the photon) with momentum greater than 1 GeV/c were required to be at least 15° away from the photon. Although some of the energy of a photon near the electromagnetic calorimeter boundaries may be deposited in the HCAL, the hadronic energy associated to the photon was required to be below 5 GeV, and to be less than half of the total photon energy.

The $W^+W^-\gamma$ sample included fully-hadronic ($q\bar{q}q\bar{q}$) and semi-leptonic ($q\bar{q}e\nu$, $q\bar{q}\mu\nu$ and $q\bar{q}\tau\nu$) candidate events in which a photon was identified. Following the procedures for the analysis of W^+W^- events described in [20], the selection of fully-hadronic final states was based on a Neural Network (NN) analysis, and that of semi-leptonic final states on an Iterative Discriminant Analysis (IDA). The efficiencies of the selections were of around 80% for the fully-hadronic events and 90%, 80% and 65% for muon, electron and tau semi-leptonic events, respectively; the purities ranged from 80% in the fully-hadronic to 99% in the muon channel. The background was composed of 75% $q\bar{q}$ events in the fully-hadronic channel and equal amounts of $q\bar{q}$ and 4-fermion events in the semi-leptonic channels. Since the selection was not tuned specifically for the $W^+W^-\gamma$ process, extra cuts were applied to reject background further, as described below.

The measured LEP beam energy values [21] were then used in kinematic fits, imposing energy-momentum conservation in the fully-hadronic channel, and imposing energy-momentum conservation and requiring that the two-jet system and the lepton-neutrino system have equal masses in the semi-leptonic channels. In all the fits performed, all the isolated photons were considered to come from outside the Ws, effectively reducing the energy available for the W^+W^- system. The χ^2 of the kinematic fits had to be below 10 and the corresponding fitted quantities were used in the subsequent analysis.

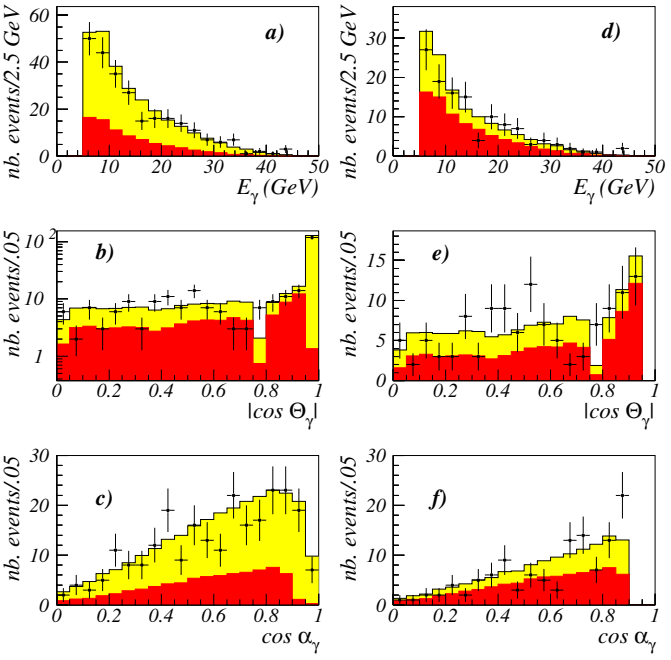

Fig. 1 a,d Distributions of energy, **b,e** cosine of the polar angle, and **c,f** cosine of the isolation angle of the photons in all data samples and all channels. **a**, **b**, and **c** show distributions of the events selected before the imposition of the signal definition cuts described in the text and **d**, **e**, and **f** the distributions after imposition of the signal cuts. The data (dots) are compared to the total SM prediction (shaded histogram). The SM $W^+W^-\gamma$ signal, generated within the phase space cuts, is shown in the darker histogram. In **c** and **f** events with isolation angle above 90° are not displayed

The maximum energy of the photon was restricted to be below $(\frac{s-(2M_W)^2}{2\sqrt{s}} - 5)$ GeV to select events above the W^+W^- threshold. In the fully-hadronic final state, the output value of the W^+W^- Neural Network was required to be larger than 0.70 for all years. In the semi-leptonic samples, the lepton and the neutrino reconstructed by the constrained fit were required to be isolated in relation to the jets by at least 10° and 5°, respectively.

4 Cross-section measurement

The numbers of events selected as $W^+W^-\gamma$ candidates, according to the criteria described above, are shown in table 1 (lines labelled "w/o PS") for each channel, dividing the data into three samples according to the year in which they were collected. The distributions of the photon energy, polar angle and isolation angle with respect to the reconstructed jets and leptons are shown in Fig. 1a–c, for these events. The agreement between data and simulation for the angular variables was checked in large samples of $q\bar{q}\gamma$ events, corresponding to radiative returns to the Z^0 pole, and no systematic differences were observed.

The measurement of the $W^+W^-\gamma$ cross-section was performed in a more restricted phase space region in which the photons fulfilled the following criteria:

– $|\cos\theta_\gamma| < 0.95$, where θ_γ is the angle between the photon and the incoming electron beam;
– $\cos\alpha_\gamma < 0.90$, where α_γ is the smallest angle between the photon and the final state charged fermions.

The above cuts were applied in addition to the previously defined criterion:

– $E_\gamma > 5$ GeV.

The same cuts were applied to the reconstructed events previously selected (the isolation angle being defined in relation to identified jets and charged leptons) and the resulting samples used both in the cross-section determination and in the anomalous couplings analysis. The numbers of events after application of these cuts are also shown in table 1 (2nd row for each data sample listed), and the distributions of the energy and angular variables of the photons in these samples are shown in Fig. 1d–f. Events with isolation angles $\alpha_\gamma > 90^\circ$ are not shown in 1c and f: after imposing the signal definition cuts there are 4 such events in data, with 3.3±0.1 expected from simulation. There is good agreement between the data and the SM expectations, except in two samples in the tau channel, where a global deficit of around 2 standard deviations with respect to the expectations is observed.

The selections for the four final states are exclusive and the efficiencies quoted in table 1 were calculated with respect to the total $W^+W^-\gamma$ sample within the signal region, thus including the branching fractions to the various decay final states. Note that these are not just the SM decay branching ratios of the $W^\pm$, as the FSR contribution is different for each final state. The selection purities (P) and efficiencies (ϵ) vary between channels and also according to the centre-of-mass energies. In the final selection, the muon sample has the highest values ($P \sim 80\%$ and $\epsilon \sim 53\%$ of the $q\bar{q}\mu\nu\gamma$ signal events), followed by the electron sample, the tau sample and the fully-hadronic sample with the lowest values ($P \sim 52\%$ and $\epsilon \sim 34\%$). The samples selected in the tau channel contain substantial contributions from the other final states, which are taken as signal.

The cross-sections were measured using a likelihood fit to the Poissonian probability for observing the numbers of events shown for each channel in the relevant rows of Table 1:

- $\sigma_{WW\gamma}(\sqrt{s} \sim 189\ \text{GeV}) = 0.19 \pm 0.09 \pm 0.02$ pb (SM: 0.340 ± 0.017 pb),
- $\sigma_{WW\gamma}(\sqrt{s} \sim 198\ \text{GeV}) = 0.44 \pm 0.09 \pm 0.03$ pb (SM: 0.385 ± 0.019 pb),
- $\sigma_{WW\gamma}(\sqrt{s} \sim 206\ \text{GeV}) = 0.34 \pm 0.09 \pm 0.03$ pb (SM: 0.421 ± 0.021 pb),

where the first errors are statistical and the second systematic. The cross-sections obtained with WPHACT/YFSWW for the SM expectations, in the same phase space region, are given with an associated 5% error [3].

Although the statistical errors are dominant, conservative systematic errors have been estimated from several sources. The effect of the signal modelling is estimated by varying the photon distributions (by changing the relative importance of FSR, from the expected 25%-30% of the signal to 0% or 50%, and of anomalous QGC contributions, within the experimentally allowed range determined in the next section), and leads to a relative error of 5% on the global efficiency. This is complemented with separate contributions of 1.5% and 3% from the uncertainty in the NN/IDA selections [20] and in the photon selection [22], respectively. A contribution from the modelling of the only significant non-4-fermion background, $q\bar{q}(\gamma)$, was obtained conservatively by varying the estimated contribution from this channel by ±20%, to take into account the uncertainties in the photon production from fragmentation and in the description of 4-jet observables [23]. The last contribution comes from the finite size of the simulation samples. All the independent contributions were added in quadrature and the correlations from the errors at different energies were neglected.

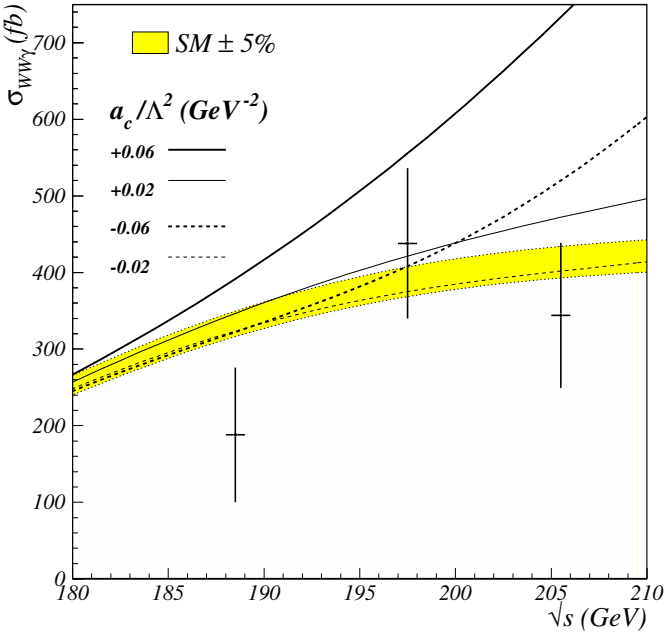

Fig. 2. $W^+W^-\gamma$ cross-section as a function of the centre-of-mass energy. The measured cross-sections (crosses) are compared to the SM prediction from WPHACT/YFSWW. The cross-sections obtained with EEWWG for indicative values of the anomalous parameter a_c/Λ^2 (in GeV^{-2}) are also shown

Figure 2 shows the comparison between the measured cross-section and the expected cross-section from WPHACT/YFSWW. The changes induced by the presence of anomalous QGCs for characteristic values of the parameters introduced in Sect. 1, calculated with EEWWG, are also shown.

Another LEP analysis [4] has introduced an extra cut requiring the two $W^\pm$ bosons to be *quasi* on-shell ($|M_{ff'} - M_W| < 2\Gamma_W$) and split the 1999 data into two samples. In that analysis, the FSR is not considered in the signal. We give corresponding results for comparison and to allow for combination of LEP results. Keeping the analysis unchanged but considering the signal defined in this way leads to a reduction of the signal to between 52% and 55% of the original value, with slightly higher efficiencies (ex-

Table 1. Number of selected events per channel for each year of data taking, compared to the expected number of events for the total SM simulation (MC_{tot}). The numbers corresponding to the contributions of 4-fermion events (and specifically of $W^+W^-\gamma$ events) to the total selected simulation sample are also shown. The two lines for each channel show the numbers of events selected as $W^+W^-\gamma$ candidates, respectively, without (labeled "w/o PS") and with the imposition of the signal phase space cuts defined in the text. The efficiency for the signal is shown in the last column for the selection within the signal phase space cuts and takes into account the branching fractions into each channel. The lower values of luminosity for the semi-leptonic samples reflect extra requirements on the detector status

Channel		Data	MC_{tot}	4-fermion	$WW\gamma$	eff×BF
1998: $\sqrt{s}$ ∼189 GeV, $\mathcal{L}$=154 pb^{-1}						
$q\bar{q}e\nu\gamma$	(w/o PS)	6	8.3±0.2	8.0±0.2	3.0±0.1	
$q\bar{q}e\nu\gamma$		4	4.0±0.2	3.8±0.1	2.9±0.1	5.5%
$q\bar{q}\mu\nu\gamma$	(w/o PS)	9	10.2±0.2	10.1±0.2	3.5±0.1	
$q\bar{q}\mu\nu\gamma$		5	4.6±0.2	4.6±0.1	3.5±0.1	6.6%
$q\bar{q}\tau\nu\gamma$	(w/o PS)	9	12.4±0.3	10.0±0.2	3.7±0.1	
$q\bar{q}\tau\nu\gamma$		1	6.4±0.3	4.9±0.2	3.6±0.1	6.8%
$q\bar{q}q\bar{q}\gamma$	(w/o PS)	25	31.3±0.6	25.3±0.4	7.9±0.2	
$q\bar{q}q\bar{q}\gamma$		11	15.8±0.4	12.6±0.2	7.6±0.2	14.5%
sum	(w/o PS)	49	62.3±0.7	53.3±0.5	18.0±0.3	
sum		21	30.7±0.5	25.8±0.4	17.5±0.3	33.5%
1999: $\sqrt{s}$ ∼198 GeV, $\mathcal{L}$=221 pb^{-1} ($q\bar{q}l\nu\gamma$) and $\mathcal{L}$=227 pb^{-1} ($q\bar{q}q\bar{q}\gamma$)						
$q\bar{q}e\nu\gamma$	(w/o PS)	11	14.5±0.3	13.6±0.2	4.8±0.1	
$q\bar{q}e\nu\gamma$		5	6.7±0.2	6.2±0.2	4.7±0.1	5.6%
$q\bar{q}\mu\nu\gamma$	(w/o PS)	15	16.1±0.3	16.0±0.3	6.2±0.2	
$q\bar{q}\mu\nu\gamma$		9	7.5±0.2	7.5±0.2	6.0±0.2	7.1%
$q\bar{q}\tau\nu\gamma$	(w/o PS)	25	22.6±0.3	18.6±0.3	6.5±0.2	
$q\bar{q}\tau\nu\gamma$		11	10.9±0.2	8.6±0.2	6.3±0.2	7.5%
$q\bar{q}q\bar{q}\gamma$	(w/o PS)	56	52.6±0.6	44.6±0.5	13.8±0.3	
$q\bar{q}q\bar{q}\gamma$		30	25.2±0.4	21.1±0.3	13.4±0.3	15.3%
sum	(w/o PS)	107	105.8±0.8	92.8±0.6	31.4±0.4	
sum		55	50.3±0.5	43.3±0.4	30.4±0.4	35.4%
2000: $\sqrt{s}$ ∼206 GeV, $\mathcal{L}$=199 pb^{-1} ($q\bar{q}l\nu\gamma$) and $\mathcal{L}$=219 pb^{-1} ($q\bar{q}q\bar{q}\gamma$)						
$q\bar{q}e\nu\gamma$	(w/o PS)	14	14.9±0.3	14.0±0.3	4.8±0.2	
$q\bar{q}e\nu\gamma$		6	6.4±0.2	6.0±0.2	4.7±0.2	5.6%
$q\bar{q}\mu\nu\gamma$	(w/o PS)	14	16.9±0.3	16.8±0.3	6.1±0.2	
$q\bar{q}\mu\nu\gamma$		6	7.2±0.2	7.2±0.2	5.9±0.2	7.0%
$q\bar{q}\tau\nu\gamma$	(w/o PS)	12	22.1±0.4	18.4±0.3	6.2±0.2	
$q\bar{q}\tau\nu\gamma$		5	10.4±0.3	8.3±0.2	6.0±0.2	7.1%
$q\bar{q}q\bar{q}\gamma$	(w/o PS)	59	58.0±0.7	49.3±0.5	14.9±0.3	
$q\bar{q}q\bar{q}\gamma$		29	27.1±0.5	22.7±0.3	14.4±0.3	15.6%
sum	(w/o PS)	99	111.8±0.9	98.6±0.7	32.1±0.4	
sum		46	51.2±0.6	44.1±0.4	30.9±0.4	35.4%

cept for the $q\bar{q}\tau\nu$ channel). The measured cross-sections in this case are:

- $\sigma_{WW\gamma}(\sqrt{s}$ ∼189 GeV) = 0.05 ±0.08 ±0.01 pb (SM: 0.176 ±0.004 pb),
- $\sigma_{WW\gamma}(\sqrt{s}$ ∼195 GeV) = 0.17 ±0.12 ±0.02 pb (SM: 0.203 ±0.004 pb),
- $\sigma_{WW\gamma}(\sqrt{s}$ ∼200 GeV) = 0.34 ±0.12 ±0.02 pb (SM: 0.217 ±0.004 pb),
- $\sigma_{WW\gamma}(\sqrt{s}$ ∼206 GeV) = 0.18 ±0.08 ±0.02 pb (SM: 0.233 ±0.005 pb).

The theoretical error on these predicted cross-sections is smaller [3] than that quoted for the previous selections because only the ISR and WSR processes are considered here.

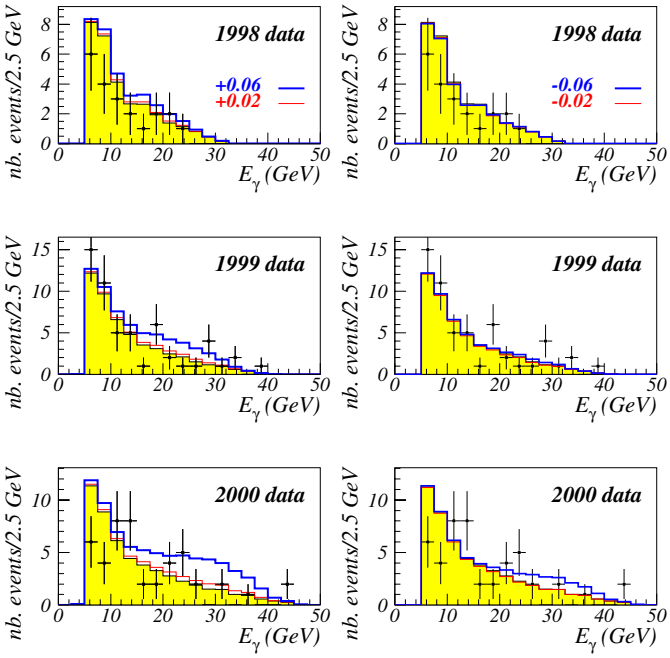

Fig. 3. Effect of anomalous couplings in the photon energy spectra in each data sample: data with $\sqrt{s}$ =189 GeV (top), data with $\sqrt{s}$ =198 GeV (middle) and data with $\sqrt{s}$ =206 GeV (bottom). The data (dots) are compared to the total SM predictions (shaded histogram). The expected distributions with anomalous QGCs are also shown for positive (left) and negative (right) values of a_c/Λ^2 (in GeV^{-2})

5 Anomalous couplings

The anomalous contributions to the quartic gauge couplings were evaluated with EEWWG in terms of the parameters a_c/Λ^2, a_0/Λ^2 and $\tilde{a}_0/\Lambda^2$, affecting $W^+W^-\gamma\gamma$ vertices, and a_n/Λ^2 and $\tilde{a}_n/\Lambda^2$, affecting $W^+W^-Z^0\gamma$ vertices. These parameters were defined in Sect. 1. The anomalous operators change not only the cross-section but also the photon energy spectra for the phase space region defined above, and their effects are stronger as the centre-of-mass energy increases. This has been seen in the variation of the total cross-section with energy displayed in Fig. 2, and is also demonstrated in Fig. 3, which shows the measured and predicted photon energy spectra for the data samples at different energies. These figures show the SM predictions and also those for four non-zero values of a_c/Λ^2; the distributions predicted for non-zero values of the other parameters show the same general behaviour. The effect on the angular variables is smaller and further reduced by the selection of central and isolated photons.

A likelihood fit to the photon energy spectra for all the individual channels and data sets gives as most probable values of the QGC parameters (in each case setting the values of the others to zero):

- $a_c/\Lambda^2 = +0.000^{+0.019}_{-0.040}$ GeV^{-2};
- $a_0/\Lambda^2 = -0.004^{+0.018}_{-0.010}$ GeV^{-2};
- $\tilde{a}_0/\Lambda^2 = -0.007^{+0.019}_{-0.008}$ GeV^{-2};
- $a_n/\Lambda^2 = -0.09^{+0.16}_{-0.05}$ GeV^{-2};
- $\tilde{a}_n/\Lambda^2 = +0.05^{+0.07}_{-0.15}$ GeV^{-2}.

Both statistical and systematic uncertainties are included (the relative contributions are the same as in the cross-section measurement). At 95% confidence level, the allowed ranges of the anomalous QGCs are constrained to be:

- -0.063 GeV$^{-2} < a_c/\Lambda^2 < +0.032$ GeV^{-2};
- -0.020 GeV$^{-2} < a_0/\Lambda^2 < +0.020$ GeV^{-2};
- -0.020 GeV$^{-2} < \tilde{a}_0/\Lambda^2 < +0.020$ GeV^{-2};
- -0.18 GeV$^{-2} < a_n/\Lambda^2 < +0.14$ GeV^{-2};
- -0.16 GeV$^{-2} < \tilde{a}_n/\Lambda^2 < +0.17$ GeV^{-2}.

The correlation between the different parameters is small and thus these results are not substantially changed when multi-parameter fits are performed. The two parameters which are CP-conserving and affect the $W^+W^-\gamma\gamma$ vertex show the largest correlation: the 95% upper confidence limit of a_0/Λ^2 is 0.025 GeV^{-2} when a_0/Λ^2 is fitted together with a_c/Λ^2.

6 Conclusions

About 600 pb^{-1} of LEP2 data, corresponding to centre-of-mass energies between 189 GeV and 209 GeV, were analysed to study the final state $W^+W^-\gamma$, where the photon is required to have E_γ >5 GeV, $|\cos\theta_\gamma|$ <0.95 and to be isolated with respect to the final state charged fermions by $\cos\alpha_\gamma$ <0.90.

The cross-sections for $W^\pm$ pair production with a photon in the final state were found to be in agreement with the SM prediction and the photon energy spectra were used to test the presence of anomalous QGCs. The data show no evidence for quartic gauge boson couplings.

Acknowledgements. We are greatly indebted to our technical collaborators, to the members of the CERN-SL Division for the excellent performance of the LEP collider, and to the funding agencies for their support in building and operating the DELPHI detector. We acknowledge in particular the support of Austrian Federal Ministry of Education, Science and Culture, GZ 616.364/2-III/2a/98, FNRS–FWO, Flanders Institute to encourage scientific and technological research in the industry (IWT), Federal Office for Scientific, Technical and Cultural affairs (OSTC), Belgium, FINEP, CNPq, CAPES, FUJB and FAPERJ, Brazil, Czech Ministry of Industry and Trade, GA CR 202/99/1362, Commission of the European Communities (DG XII), Direction des Sciences de la Matière, CEA, France, Bundesministerium f"ur Bildung, Wissenschaft, Forschung und Technologie, Germany, General Secretariat for Research and Technology, Greece, National Science Foundation (NWO) and Foundation for Research on Matter (FOM), The Netherlands, Norwegian Research Council, State Committee for Scientific Research, Poland, SPUB-M/CERN/PO3/DZ296/2000, SPUB-M/CERN/PO3/DZ297/2000 and 2P03B 104 19 and 2P03B 69

23(2002-2004) JNICT–Junta Nacional de Investigação Científica e Tecnológica, Portugal, Vedecka grantova agentura MS SR, Slovakia, Nr. 95/5195/134, Ministry of Science and Technology of the Republic of Slovenia, CICYT, Spain, AEN99-0950 and AEN99-0761, The Swedish Natural Science Research Council, Particle Physics and Astronomy Research Council, UK, Department of Energy, USA, DE-FG02-01ER41155, EEC RTN contract HPRN-CT-00292-2002.

References

1. ALEPH, DELPHI, L3 and OPAL Collaborations, the LEP Electroweak Working Group and the SLD Heavy Flavour Group, "A Combination of Preliminary Electroweak Measurements and Constraints on the Standard Model", CERN EP/2002-091, hep-ex/0212036 (2002).
2. G. Bélanger and F. Boudjema, Phys. Lett. B **288**, 210 (1992); O.J.P.Éboli, M.C. Gonzalez-Garcia and S.F. Novaes, Nucl. Phys. B **411**, 381 (1994); G. Bélanger et al., Eur. Phys. J. C **13**, 283 (2000).
3. A. Denner, S. Dittmaier, M. Roth and D.Wackeroth, Eur. Phys. J. C **20**, 201 (2001).
4. L3 Collaboration, P. Achard et al., Phys. Lett. B **527**, 29 (2002).
5. OPAL Collaboration, G. Abbiendi et al., Phys. Lett. B **471**, 293 (1999).
6. DELPHI Collaboration, P. Aarnio et al., Nucl. Instr. and Meth. A **303**, 233 (1991).
7. DELPHI Collaboration, P. Abreu et al., Nucl. Instr. and Meth. A **378**, 57 (1996).
8. DELPHI Silicon Tracker group, P. Chochula et al., Nucl. Instr. and Meth. A **412**, 304 (1998).
9. A. Ballestrero, R. Chierici, F. Cossutti and E. Migliore, Comp. Phys. Comm. **152**, 175 (2003).
10. E. Accomando and A. Ballestrero, Comp. Phys. Comm. **99**, 270 (1997); E. Accomando, A. Ballestrero and E. Maina, Comp. Phys. Comm. **150**, 166 (2003).
11. S. Jadach et al., Comp. Phys. Comm. **140**, 432 (2001).
12. T. Sjöstrand et al., Comp. Phys. Comm. **135**, 238 (2001).
13. S. Jadach *el al.*, Comp. Phys. Comm. **76**, 361 (1993).
14. E. Barberio and Z. Wąs, Comp. Phys. Comm. **79**, 291 (1994).
15. S. Jadach, B.F.L. Ward and Z.Wąs, Comp. Phys. Comm. **130**, 260 (2000).
16. DELPHI Coll., P. Abreu et al., Zeit. Phys. C **73**, 11 (1996).
17. W.J. Stirling and A. Werthenbach, Eur. Phys.J. C **14**, 103 (2000).
18. F.A. Berends, R. Pittau and R. Kleiss, Nucl. Phys. B **426**, 344 (1994).
19. W. Beenakker et al., *WW cross-section and distributions*, Physics at LEP2, eds. G. Altarelli, T. Sjöstrand and F. Zwirner, CERN 96-01 (1996) Vol 1, 79.
20. DELPHI Collaboration, "Measurement of the W-pair production cross-section and W Branching Ratios in e^+e^- collisions at $\sqrt{s} = 161 - 209$ GeV", to be submitted to EPJC.
21. The LEP Energy Working Group, A. Blondel et al., Eur. Phys. J. C **11**, 573 (1999).
22. DELPHI Collaboration, P. Abreu et al., Phys. Lett. B **491**, 67 (2000).
23. M.W. Grünewald et al., "LEP2 Monte Carlo Workshop: Report of the Working Groups on Precision Calculations for LEP2 Physics", CERN 2000-009 (2000), hep-ph/0005309.